Neuro-Oncology

Neuro-Oncology 17(4), 545–554, 2015
doi:10.1093/neuonc/nou234
Advance Access date 24 September 2014

Effective treatment of diverse medulloblastoma models with mebendazole and its impact on tumor angiogenesis

Ren-Yuan Bai, Verena Staedtke, Charles M. Rudin, Fred Bunz, and Gregory J. Riggins

Department of Neurosurgery (R.-Y.B., G.J.R.), Department of Neurology (V.S.); Department of Radiation Oncology, Johns Hopkins University School of Medicine, Baltimore, Maryland (F.B.); Department of Thoracic Oncology, Memorial Sloan Kettering Cancer Center, New York, New York (C.M.R.)

Corresponding Authors: Gregory J. Riggins or Ren-Yuan Bai, PhD, Department of Neurosurgery, Johns Hopkins University, Koch Building Rm. 257, 1550 Orleans Street, Baltimore, MD 21231 (griggin1@jhmi.edu or rbai1@jhmi.edu).

Background. Medulloblastoma is the most common malignant brain tumor in children. Current standard treatments cure 40%–60% of patients, while the majority of survivors suffer long-term neurological sequelae. The identification of 4 molecular groups of medulloblastoma improved the clinical management with the development of targeted therapies; however, the tumor acquires resistance quickly. Mebendazole (MBZ) has a long safety record as antiparasitic in children and has been recently implicated in inhibition of various tyrosine kinases in vitro. Here, we investigated the efficacy of MBZ in various medulloblastoma subtypes and MBZ's impact on vascular endothelial growth factor receptor 2 (VEGFR2) and tumor angiogenesis.

Methods. The inhibition of MBZ on VEGFR2 kinase was investigated in an autophosphorylation assay and a cell-free kinase assay. Mice bearing orthotopic *PTCH1*-mutant medulloblastoma allografts, a group 3 medulloblastoma xenograft, and a *PTCH1*-mutant medulloblastoma with acquired resistance to the smoothened inhibitor vismodegib were treated with MBZ. The survival benefit and the impact on tumor angiogenesis and VEGFR2 kinase function were analyzed.

Results. We determined that MBZ interferes with VEGFR2 kinase by competing with ATP. MBZ selectively inhibited tumor angiogenesis but not the normal brain vasculatures in orthotopic medulloblastoma models and suppressed VEGFR2 kinase in vivo. MBZ significantly extended the survival of medulloblastoma models derived from different molecular backgrounds.

Conclusion. Our findings support testing of MBZ as a possible low-toxicity therapy for medulloblastomas of various molecular subtypes, including tumors with acquired vismodegib resistance. Its antitumor mechanism may be partially explained by inhibition of tumor angiogenesis.

Keywords: angiogenesis, mebendazole, medulloblastoma, VEGF, VEGFR2.

Medulloblastoma, the most common type of pediatric brain malignancy, is an aggressive primitive neuroectodermal tumor arising from the cerebellum. The incidence peaks twice during childhood: at 3–4 years of age and at 8–9 years of age. Despite an increased molecular understanding and significant improvements in therapy, only slightly more than half of children with the diagnosis of medulloblastoma survive >10 years. Current treatments combining surgery, radiotherapy, and antiproliferative chemotherapy have been successful, but these treatments can have long-lasting adverse effects, including impaired neural development.[1] In particular, radiation therapy causes late effects such as neurocognitive deficiencies, hormone deficits, and growth impairment.[1] The most common chemotherapy-related late effects are ototoxicity caused by platinum drugs, secondary leukemia, and infertility following exposure to alkylating agents.[1] Since the present therapy does not address about 40% of patients who still succumb to the disease,[2] and the surviving patients risk severe side effects, less toxic and more efficacious therapy is needed.

Recent studies have demonstrated that medulloblastoma comprises several molecularly distinct groups based on the specific genetic alterations and on the gene expression profiles. The Wnt group is typified by a gene expression signature of activated Wnt signaling, and a sonic hedgehog (SHH) group is defined by the expression of genes downstream of the hedgehog (Hh) pathway, by mutations in *PTCH1*, the Hh pathway tumor suppressor, and by mutations in *p53*. Group 3 has the worst prognosis and is often associated with MYC amplification and overexpression,

Received 25 March 2014; accepted 17 August 2014

while group 4 medulloblastoma presents an intermediate prognosis and sometimes is associated with cyclin-dependent kinase (CDK)6 or MYCN amplifications.[2,3]

The molecular or genetic basis of certain medulloblastoma groups may sensitize them to targeted therapy. This was demonstrated by the effectiveness of the Hh-pathway inhibitor vismodegib (GDC-0449), an orally bioavailable small-molecule inhibitor of smoothened (SMO), on a patient with a disseminated SHH group medulloblastoma.[4] Unfortunately, in this patient, prolonged treatment with vismodegib eventually failed, as recurrent tumor had acquired mutations in SMO.[4,5] This case study illustrates the risk of targeting a mutable onco-pathway and a genetically diverse tumor cell population.

Compared with other solid tumors, brain tumors are especially difficult to treat, owing mainly to insufficient drug delivery to intracranial tumors. Many chemotherapeutics that are effective against brain tumor cells in vitro fail to reach effective concentrations in the intracranial tumor.[6] In the pediatric patient population, drug-related neural toxicity to the developing brain further limits options.

Mebendazole (MBZ) is an antiparasitic drug with a long history of safe human use against helminthic infections, even at high doses. Recently, we discovered MBZ as a potent drug in treating orthotopic glioma in mice with low toxicity.[7] GBM is a highly aggressive brain tumor, and MBZ was able to significantly improve the animals' survival.

MBZ is a benzimidazole, with a low molecular weight of 295 daltons and a high degree of lipophilicity contributing to brain permeability.[8] MBZ binds to tubulin and disrupts the formation of microtubules that are essential in a broad range of cellular functions, such as the formation of mitotic spindle and cytoskeleton. In recent years, several mechanisms have been proposed for MBZ's antitumor activity, including B-cell lymphoma 2 inactivation and downregulation of X-linked inhibitor of apoptosis protein.[9,10] We have previously reported that MBZ disrupts microtubules in glioma cells and MBZ can be efficacious in intracranial gliomas with oral administration.[7] Even though tubulin is a well-known anticancer target, further details of the molecular mechanism of MBZ's antitumor activity in brain tumors have not yet been determined. Recently, Dakshanamurthy and colleagues[11] applied a computational proteo-chemometric method with a library of FDA-approved compounds and identified MBZ as one potential inhibitor of vascular endothelial growth factor receptor 2 (VEGFR2), which suggested a possible role of MBZ in interfering with tumor angiogenesis.

In this study, we characterized the inhibition of VEGFR2 kinase by MBZ and demonstrated that MBZ exhibited an anti-angiogenic effect and interfered with VEGFR2 activity in multiple medulloblastoma models. We showed that MBZ extended survival in intracranial models of the SHH group and group 3 medulloblastoma.

Materials and Methods

Cell Lines and Tissue Culture

Medulloblastoma cell line D425Med (D425) was obtained from the Duke University Brain Tumor Center. UW228 was obtained from Dr J. R. Silber at the University of Washington.[12] Cells were maintained in Dulbecco's modified Eagle's medium (DMEM) supplemented with 10% fetal bovine serum and antibiotics. Cells were kept in frozen stocks upon reception and were not additionally authenticated. Human umbilical vein endothelial cells (HUVECs) obtained from American Type Culture Collection (passage 3) were maintained in DMEM supplemented with 10% fetal bovine serum and antibiotics with the addition of 50 μg/mL endothelial cell growth supplement from Sigma. Tissue culture was maintained at 37°C in humidified air containing 5% CO_2.

Luciferase Expression by Lentivirus

The firefly luciferase cDNA from pGL3-basic (Promega) was subcloned in pFUGW and transfected along with CMVΔR8.91 and pMD.G in 293T cells by Lipofectamine 2000 (Invitrogen). Virus was harvested after 48 h, and D425 cells were infected by incubating with 8 μg/mL polybrene (Sigma) in the growth medium. The allograft tumor cells were infected by incubating with luciferase lentivirus at room temperature for 10 min.

Animal Experiments

All animal work was approved by the Animal Care and Use Committee of Johns Hopkins University.

The parental mouse medulloblastoma allograft model was derived from spontaneous medulloblastoma in patched (PTCH)+/−, p53−/− mice, and propagated as subcutaneous allografts in athymic nude mice.[13] Vismodegib (GDC-0449)-resistant allografts expressing SMO-D477G (SG274) were derived from parental allografts following the treatment of vismodegib as previously described.[5]

Female athymic nude mice, 5–6 weeks of age, were purchased from the National Cancer Institute. For the implantation procedure, female athymic nude mice were anesthetized via intraperitoneal injection of 60 μL of a stock solution containing ketamine hydrochloride (75 mg/kg) (100 mg/mL; Abbot Laboratories), xylazine (7.5 mg/kg) (100 mg/mL; Xyla-ject, Phoenix Pharmaceutical), and ethanol (14.25%) in a sterile 0.9% NaCl solution. D425 cells infected with luciferase lentivirus were prepared by centrifugation at 125 *g* for 6 min at 4°C. Allograft tumors were first implanted subcutaneously in a nude mouse. When the tumor reached 300–1000 mm^3, the mouse was euthanized and the tumor was processed by first mincing and then incubating with 2.5 mg/mL collagenase and 500 unit/mL hyaluronidase (Sigma) at 37°C and 200 rpm for 15 min. The tissues were then passed through a 70-μm cell strainer and washed with phosphate buffered saline (PBS) 3 times before the implantation. Using a stereotactic frame, 500 000 D425 cells or 100 000 PTCH+/−, p53−/− allograft cells were injected through a burr hole drilled 1 mm right of the midline and 1 mm posterior to the lambdoid suture, at a depth of 2.5 mm below the dura at a rate of 1 μL/min.

At day 5 post-implantation of the tumor cells, MBZ was administered by daily oral gavage as described previously.[7] MBZ tablets (Aurochem) were ground, resuspended in PBS, and mixed with 50% sesame oil (Sigma) to achieve better gastrointestinal absorption of the drug.[14] Control animals were fed with PBS mixed with 50% sesame oil. Animals were observed daily for any signs of deterioration, neurotoxicity, or movement disorders as well as weight loss. They were inspected for signs of pain and distress, as per the Johns Hopkins Animal Care and Use Guidelines. If the

symptoms persisted and resulted in debilitation, the moribund animals were euthanized according to protocol. The brain and other organs were dissected and placed in formalin for further pathological studies.

Intracranial luciferase activity was determined by a Xenogen instrument (IVIS 200) with intraperitoneal injection of 2 mg/mouse D-luciferin potassium salt solution (Gold Biotechnology). After 15 min following the injection, the animals were scanned for 1 min at a distance of 20 cm.

Vascular Endothelial Growth Factor Receptor 2 Kinase Assay

The VEGFR2 kinase activity with MBZ was measured with the VEGFR2 (kinase insert domain receptor) Kinase Enzyme System in combination with the ADP-Glo Kinase Assay (Promega). A purified fragment of human VEGFR2 (aa789-1356) containing the intracellular part including the kinase domains of VEGFR2 was used in the assay. In the half-maximal inhibitory concentration (IC_{50}) assay and time course, 20 ng VEGFR2 kinase, 1 μg poly (Glu_4,Tyr_1) peptide, 50 μM ATP, and 50 μM dithiothreitol were used in a reaction volume of 25 μL at room temperature for 60 min with various concentrations of MBZ. MBZ was dissolved in dimethyl sulfoxide, and 2.5 μL MBZ or dimethyl sulfoxide was added to each reaction. In the ATP gradient assays, 0, 2, 3, 5, 10, 50, 500 μM, or 2 or 4 mM ATP was used with 1 μg poly (Glu_4,Tyr_1) peptide in the same reaction condition. In the poly (Glu_4,Tyr_1) peptide gradient assays, 0, 0.0025, 0.005, 0.01, 0.04, or 0.4 μg/μL peptide was used with 50 μM ATP. Following the reaction, a stop solution was added to terminate the reaction

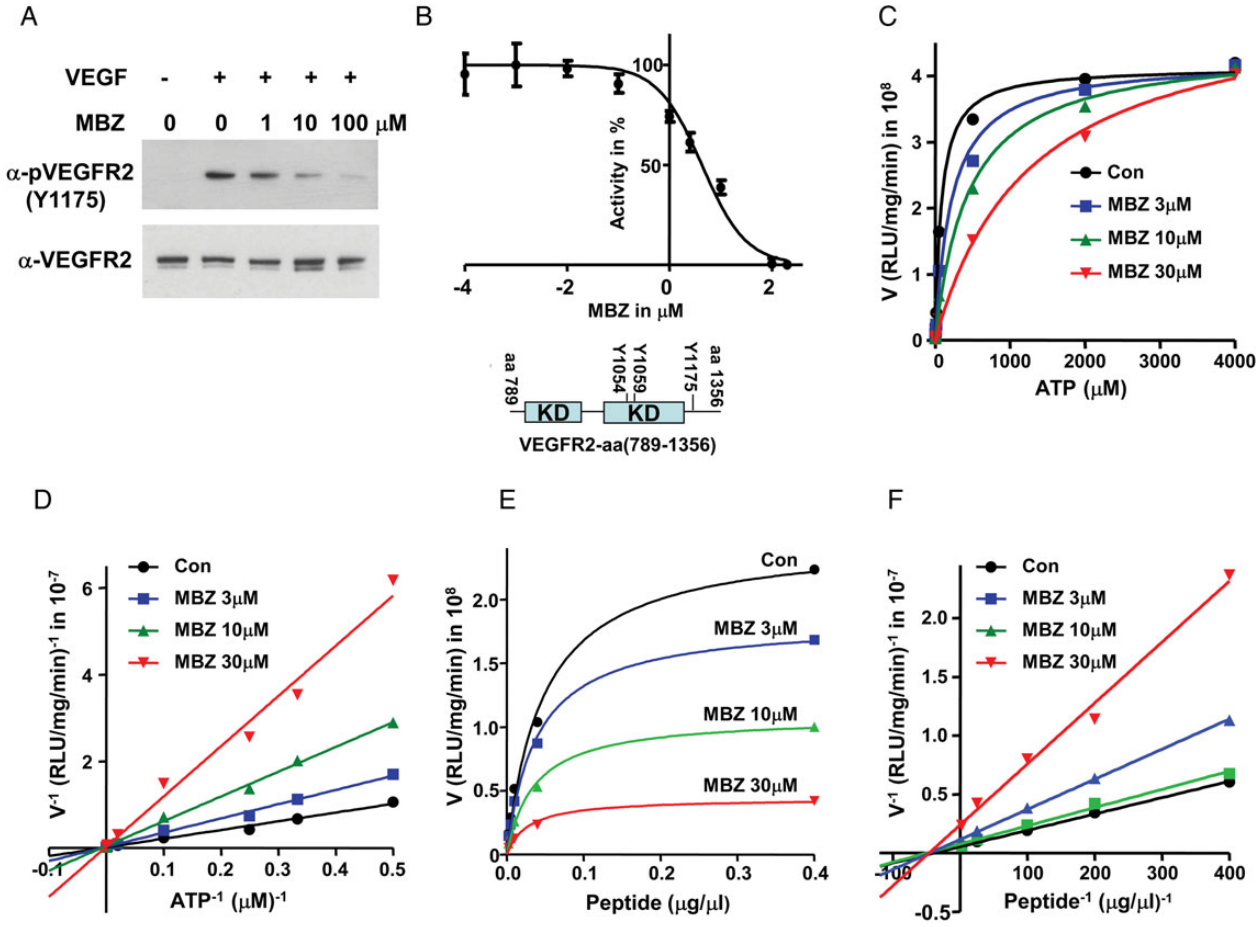

Fig. 1. MBZ inhibits VEGFR2 kinase activity and competes with ATP. (A) MBZ inhibited the autophosphorylation of VEGFR2-Y1175 in HUVECs. HUVECs were starved and treated with MBZ 30 min prior to the stimulation of 50 ng/mL VEGF. Western blot of anti-pVEGFR2-Y1175 antibody indicated the autophosphorylation of tyrosine 1175, and the levels of VEGFR2 were reflected by the anti-VEGFR2 western blot. (B) Cell-free kinase assay with a purified VEGFR2 (aa789-1356) revealed an IC_{50} of MBZ at 4.3 μM. Three measurements were performed. KD, kinase domain; Y1054/Y1059/Y1175: 3 of the major autophosphorylation sites of VEGFR2. (C, D) Effect of MBZ on the kinetics of VEGFR2 kinase activity with the ATP gradient. Kinase assays were performed with 1 μg poly (Glu_4,Tyr_1) peptide and 0, 2, 3, 5, 10, 50, 500, 2000, or 4000 μM ATP. The reactions with 0 μM ATP served as background. On the V^{-1} and ATP^{-1} plot (D), the linear regressions of the reactions with Con, 3, 10, and 30 μM MBZ converge closely within the statistic deviations at the intersection with the *y*-axis at 0.013, 0.024, 0.045, and 0.028 ($\times 10^{-7}$), respectively. (E, F) Effect of MBZ on the kinetics of VEGFR2 kinase activity with the poly (Glu_4,Tyr_1) peptide gradient. Kinase assays were performed with 50 μM ATP and 0, 0.0025, 0.005, 0.01, 0.04, or 0.4 μg/μL poly (Glu_4,Tyr_1) peptide. The activities at 0 μg/μL poly (Glu_4,Tyr_1) peptide presumably reflected the autophosphorylation of VEGFR2. The reactions without VEGFR2 kinase with 50 μM ATP, peptide, and MBZ (0, 3, 10, or 30 μM) were used as the background controls.

and deplete the remaining ATP. The subsequent ADP-Glo kinase assay detected the ADP created by the kinase reaction via a luminescence plate reader (PerkinElmer VICTOR3) on a 96-well plate with white bottoms. In the ATP gradient assay, the reactions with 0 μM ATP at various concentrations of MBZ were used as background. The kinase activities at 0 μg/μL peptide presumably reflected the autophosphorylation of VEGFR2. Enzyme kinetic data were analyzed by GraphPad Prism 5 using linear regression or nonlinear regression of Michaelis–Menten kinetics. IC_{50} data were analyzed by the same program following a procedure of transformation, normalization, and nonlinear fitting.

Western Blots

Cells were lysed in the lysis buffer as described previously.[15] HUVECs were starved in media without endothelial cell growth supplement for 5–6 h and incubated with MBZ for 30 min before being treated with 50 ng/mL recombinant human $VEGF_{165}$ (PeproTech) for 5 min at 37°C. Cell lysates were heated at 95°C for 5 min with LDS Sample Buffer (Invitrogen) supplemented with 100 mm dithiothreitol before loading onto a 4%–12% NuPAGE Bis-Tris gel (Invitrogen). After the transfer to a polyvinylidene difluoride membrane (Bio-Rad), immunostaining was performed according to standard procedure. Signals were visualized by the SuperSignal chemiluminescent system (Pierce).

Antibodies

The following antibodies were used in this study: rabbit anti-VEGF antibody (ABS82, Millipore), rabbit anti-VEGFR2 antibody (#2479, Cell Signaling Technology), mouse anti-VEGFR2 antibody (clone CH-11, Millipore), rabbit anti-pVEGFR2-Y1175 antibody (#2478, Cell Signaling Technology), rabbit anti-pVEGFR2-Y1054/1059 antibody (AB5473, Abcam), and hamster anti-CD31 antibody (MAB1398Z, Millipore).

Immunofluorescence Staining

Staining followed the procedure previously described.[16] The paraffin-embedded slides were deparrafinized using a standard procedure and treated with antigen retrieval citra solution (BioGenex). The sections were incubated with the primary antibodies as

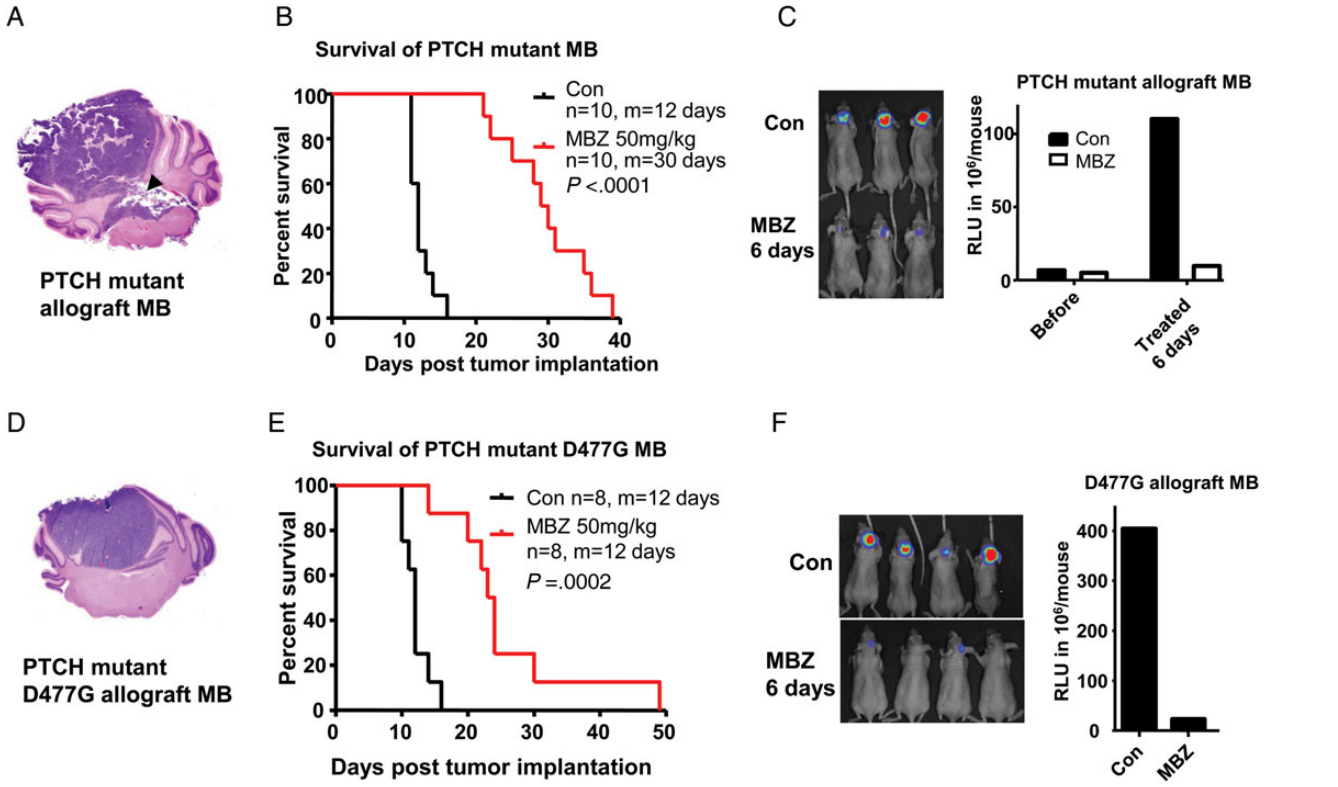

Fig. 2. MBZ inhibited the orthotopic PTCH+/−, p53−/− allograft and the vismodegib-resistant SMO-D477G medulloblastoma in mice. (A) The PTCH+/−, p53−/− allograft tumor was implanted in the right vermis of the cerebellum of nude mice. An H&E slide shows a fully grown medulloblastoma (MB) that broke into the fourth ventricle (black arrowhead). (B) Treatment with 50 mg/kg MBZ via oral gavage starting from day 5 after tumor implantation improved the median (m) survival by 150% vs the control group. (C) Xenogen scan demonstrated that the tumor growth was significantly inhibited by MBZ treatment. The tumor load in a set of representative mice after 6 days of MBZ treatment is displayed in the left picture. The right graph shows the average xenogen counts before and after the MBZ treatment. (D) D477G mutant allograft derived from a PTCH+/−, p53−/− medulloblastoma-bearing mouse treated with the Hh inhibitor vismodegib was implanted in the cerebellum of nude mice. The H&E slide shows the tumor growth in the right vermis of the cerebellum. (E) Daily treatment of mice with MBZ extended the median (m) survival from 12 days to 30 days. (F) Xenogen scan shows the inhibition of tumor growth following 6 days of MBZ treatment. The right graph shows the average xenogen counts without (Con) and with MBZ treatment.

described above and subsequently with Alexa Fluor 488 (green) or 594 (red) secondary antibodies (Invitrogen) in 10% goat serum in PBS at the room temperature, and washed 3 times in PBS in-between and after. Following the staining, the slides were covered with mounting medium containing 4′,6′-diamidino-2-phenylindole (DAPI; Vector Laboratories) and examined on a Zeiss Observer.Z1 fluorescence microscope equipped with an AxioCam MRm charge-coupled device camera. Scale bars were calculated by Adobe Photoshop CS5.5.

The microvessel density of CD31-stained slides was counted in 5 independent samples of each group as described before.[17] Briefly, each slide was viewed with ×40 magnification to identify the "hotspots" of vessels. The microvessels were counted within each area at ×200 magnification. In addition to the morphologically identifiable vessels, each immunoreactive endothelial cell cluster within the selected field was counted as one vessel. The microvessel density in normal brain tissues was counted similarly as described above, except that no "hotspot" but normal brain tissues in anatomically comparable sites distant from the tumor were selected in the treated and untreated tumor sections.

Statistical Analysis

The results are presented as a mean value plus or minus the standard deviation. Data were analyzed by GraphPad Prism 5.0. The *P*-values were determined by a Mantel–Cox test. $P < .05$ was accepted as statistically significant.

Results

MBZ Inhibits VEGFR2 Activity in a Kinase Assay and Competes With ATP

VEGFR2 is the predominant functional receptor mediating most of the cellular responses of VEGF.[18] Upon VEGF binding, VEGFR2 undergoes autophosphorylation and activates downstream signaling pathways. In HUVECs upon VEGF stimulation, the autophosphorylation of VEGFR2-Y1175 was inhibited starting with 1 μM MBZ and significantly reduced at 10 μM (Fig. 1A). Y1175 is a major autophosphorylation site of VEGFR2, which provides a binding site for the p85 subunit of phosphatidylinositol-3 kinase (PI3K) and phospholipase C gamma (PLCγ), as well as Shb.[19,20] In order to study the kinetics of this inhibition, we examined the interference of MBZ with the kinase activity of purified VEGFR2 (aa789-1356) that contains the intracellular domain. In this kinase reaction, ATP and poly (Glu_4,Tyr_1) peptide were provided as substrates. The inhibitory IC_{50} was determined at 4.3 μM (Fig. 1B), which is consistent with the inhibition of VEGFR2-Y1175 autophosphorylation at 1–10 μM MBZ detected in HUVECs. The

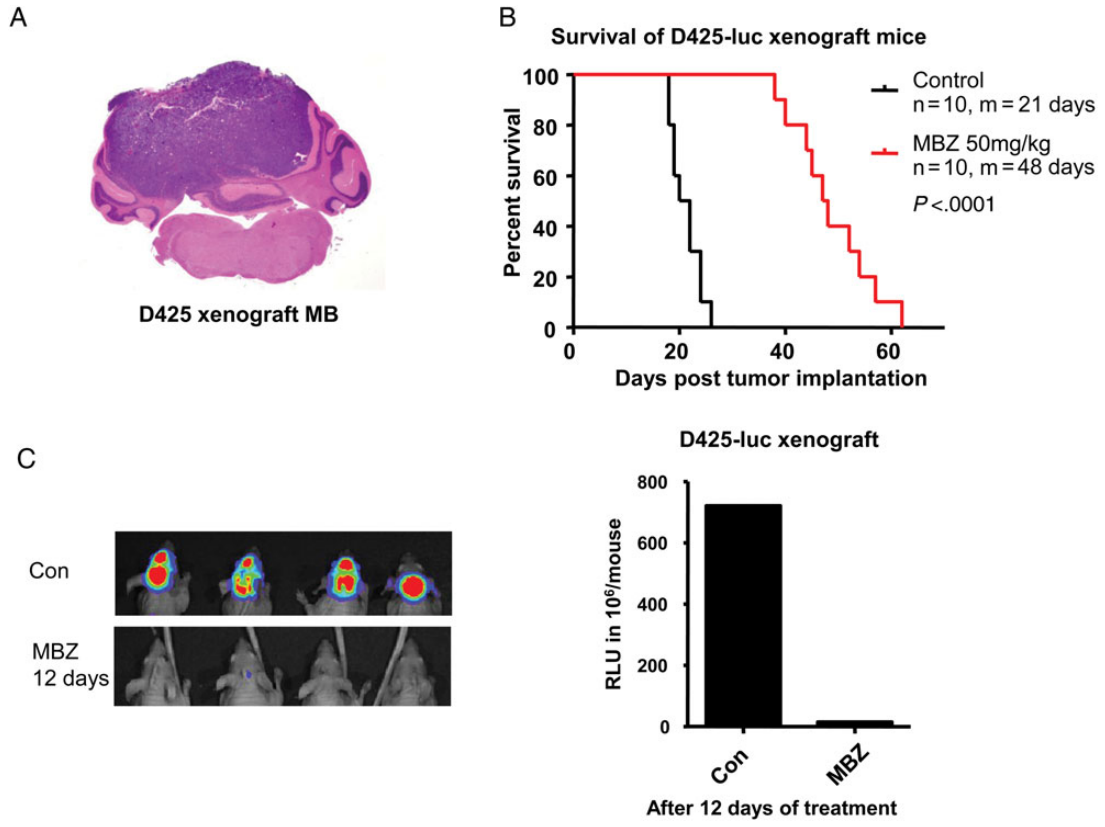

Fig. 3. MBZ markedly extended the survival of D425 xenograft medulloblastoma of group 3. (A) D425 medulloblastoma (MB) cells belong to group 3 of molecular classification and carry c-*MYC* and *OTX2* genomic amplification. The cells were implanted into the right vermis of the cerebellum of nude mice. H&E staining demonstrated the fully grown cerebellar tumor. (B) Treatment by MBZ starting from day 5 of tumor implantation improved the median (m) survival from 21 to 48 days by 129%. (C) Xenogen scan demonstrated the inhibition of tumor growth after 12 days of MBZ treatment. The right graph shows the average xenogen counts without (Con) and with MBZ treatment.

reaction occurred at a linear rate up to 60 min with or without MBZ (Supplementary Fig. S1). The kinetic study revealed that MBZ competes with ATP (Fig. 1C and D), but not with poly (Glu_4, Tyr_1) peptide in this tyrosine kinase reaction (Fig. 1E and F).

MBZ Is Highly Efficacious in PTCH+/−, p53−/− Allograft and the Vismodegib-Resistant Model

The parental PTCH+/−, p53−/− allograft was originated from a spontaneous intracranial medulloblastoma that carries the molecular and pathological features of human medulloblastoma with a mutated PTCH and aberrant Hh pathway (SHH subtype).[21] This tumor has a wild-type SMO and is initially responsive to vismodegib, a SMO inhibitor. Upon prolonged treatment of serially passaged tumor with vismodegib, a resistant population with mutated SMO-D477G emerged, closely resembling molecularly and clinically the acquired vismodegib resistance in a medulloblastoma patient.[4,5] Parental allografts and SMO-D477G mutant allografts were implanted in the mouse cerebellum, where the tumors grew in a confined manner with occasional breakout into the fourth ventricle as shown in Fig. 2A, a close resemblance to the common progression of human medulloblastoma. Five days after implantation, mice were treated with 50 mg/kg MBZ by daily gavage. This dose was selected based on our prior study that identified 50 mg/kg as the maximal tolerated dose of daily gavage.[7] The treatment improved the survival of the mice by 150% and 100% in the parental and SMO-D477G allografts, respectively (Fig. 2B and E). Luminescence images after 6 days of treatment confirmed that the tumor growth in the brain was significantly slowed by MBZ (Fig. 2C and F). These findings indicate that MBZ can be effective in the SHH group of medulloblastoma, and potentially in patients with recurrent disease following the targeted therapy.

MBZ Is Efficacious in D425 Medulloblastoma

D425 is a human medulloblastoma cell line that carries the genomic amplification of c-*MYC* and *OTX2*, and therefore belongs to group 3.[3,16,22,23] Previous studies have demonstrated that OTX2 mediates tumorigenicity of D425 in vitro and in vivo.[16,23,24] In this study, orthotopic D425 xenograft represents a medulloblastoma model distinct from the SHH group. MBZ was able to prolong the median survival of D425 xenograft mice from 21 days to 48 days, a 129% increase (Fig. 3B). At day 12 of the treatment, mice displayed significantly less tumor burden than the control animals, as reflected by the luciferase signals (Fig. 3C). In the control group, tumor cells appeared to have spread into the ventricles during the terminal stage, which gave luciferase signals in the frontal brain of the three mice on the left side (Fig. 3C, Control [Con], left panel).

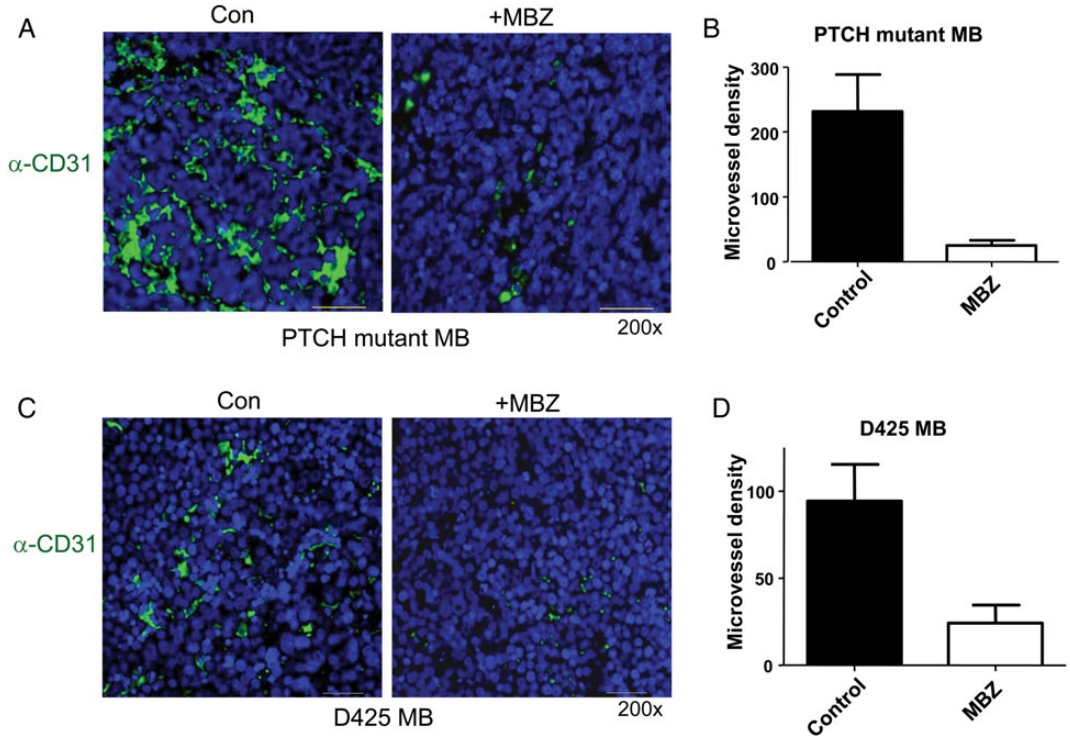

Fig. 4. MBZ reduced the formation of tumor vessels in the PTCH mutant allograft and D425 xenograft medulloblastoma. (A) The sections of PTCH mutant allograft (PTCH+/−, p53−/−) medulloblastoma (MB) were stained with anti-CD31 antibody and green fluorescent secondary antibody. Nuclei were stained with DAPI (blue). Microvessel density was counted on 200× fields ("hotspot") in 5 independent slides in each group, graphed in (B). The same frames of green fluorescence pictures were observed with the Texas Red fluorescence filter, in order to rule out possible autofluorescence. All pictures were taken with the setting of 800 msec exposure to green fluorescence and 200 msec to DAPI channel. All scale bars are 30 μm. (C, D) Similar staining and measurement were performed with D425 medulloblastoma xenografts.

MBZ Impaired Tumor Angiogenesis in Medulloblastoma Models

By comparing the mouse tumor sections, untreated and treated by MBZ, obtained at the similar terminal stage of the tumor growth, we observed a lack of tumor hemorrhages and vasculatures in the MBZ-treated tumors. This feature is particularly striking in the PTCH mutant allograft, where the untreated tumors usually showed hypervasculature and widespread hemorrhage at the terminal stage, whereas the MBZ-treated tumors lacked such appearance in the hematoxylin and eosin (H&E)–stained sections (Supplementary Fig. S2). Tumor blood vessels are mostly deficient in maturation and structural integrity, and spontaneous intratumoral hemorrhages often occur in brain and other hypervasculated tumors.[25–28]

In order to quantify the tumor vasculatures, we measured microvessel density on sections stained with the anti-CD31 antibody. CD31 (platelet endothelial cell adhesion molecule 1) is a pan-endothelial marker useful for immunohistochemical assessment of vasculature.[29] PTCH+/−, p53−/− allograft medulloblastoma exhibited intense staining with the CD31 antibody (Fig. 4A). The pronounced tumor vasculatures were greatly reduced by MBZ treatment (Fig. 4A and B). The neovasculature of D425 medulloblastoma was also significantly decreased by MBZ treatment (Fig. 4C and D). In contrast, the normal blood microvessels in the distant brain parenchyma appeared to be unaffected by MBZ, as indicated by the similar microvessel density in both animal models (Fig. 5).

MBZ Inhibits VEGFR2 Kinase Activity in Mouse Medulloblastoma

VEGF can be expressed by tumor and stromal cells and has multiple functions in tumorigenesis, including tumor angiogenesis, vascular permeability, and maintenance of cancer stem cells.[18] VEGFR2 is the predominant functional receptor mediating most of the cellular responses of VEGF.[18] Upon VEGF stimulation, VEGFR2 undergoes autophosphorylation and phosphorylates downstream signaling partners, in which Y1175 provides a binding site for PLCγ and the p85 subunit of PI3K, whereas Y1054 and Y1059 are major autophosphorylation sites in the tyrosine kinase catalytic domain that are important for the activation of VEGFR2.[19,20] We found that PTCH+/−, p53−/− allograft medulloblastoma expressed VEGF regardless of MBZ treatment, as shown by immunohistochemical staining (Fig. 6A). Despite the presence of VEGF ligand, MBZ-treated allografts displayed marked decrease of VEGFR2 activity in comparison with the control, as shown by the immunofluorescent staining of VEGFR2-Y1175 and -Y1054/1059 autophosphorylation (Fig. 6B and C). This result indicates that the tyrosine kinase function of VEGFR2 was indeed inhibited by MBZ in the treated tumors. Among the other possible antitumor mechanisms of MBZ, tubulin targeting was evident in some medulloblastoma cells, but not in D425 cells. Tubulin polymerization assays showed no interference of tubulin polymerization in D425 cells by MBZ at 1 μM, a concentration where polymerized tubulin was reduced in UW228 medulloblastoma cells (Supplementary Fig. S3A and B)

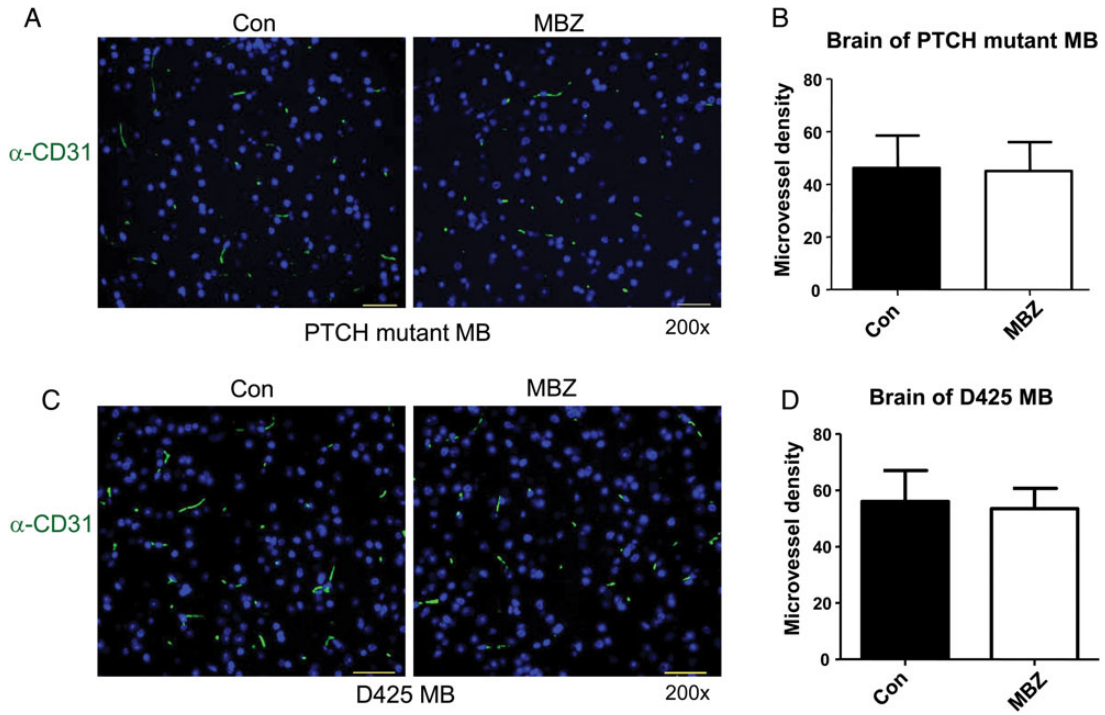

Fig. 5. MBZ did not affect the normal vasculature in the brain tissues. The sections of mouse cerebellum bearing the PTCH mutant allograft (A) or D425 xenograft tumor (C) were stained with anti-CD31 antibody and green fluorescent secondary antibody, with DAPI staining the nuclei. All scale bars are 30 μm. The microvessels in the normal brain tissues on anatomically comparable sites distant from the respective tumors are counted and graphed in (B) and (D). The microvessel density was not affected by MBZ treatment. Five independent sections were used for each group.

and in the 060919 glioblastoma cell line as previously reported.[7] Higher concentration of MBZ over the incubation time of 24 h could complicate the assay due to the excessive cell death. IC_{50} values of MBZ with a panel of medulloblastoma cells were determined to be between 0.13 and 1 μM (Supplementary Table S1), comparable to those with the glioblastoma cells.[7] A recent study by Nygren et al[30] demonstrated the inhibition of a number of tyrosine kinases by MBZ in vitro, which prompted us to examine MBZ's interference with other kinases, such as platelet derived growth factor receptor alpha (PDGFRα), in medulloblastoma. In vitro assay in NIH3T3 cells stimulated by PDGF-AA revealed the inhibition of PDGFRα-Y754 autophosphorylation by MBZ (Supplementary Fig. S4A). However, among the cells expressing it, PDGFRα was rarely autophosphorylated in PTCH+/−, p53−/− allograft medulloblastoma (Supplementary Fig. S4B). The impact of MBZ's inhibition on other tyrosine kinases, including PDGFRs on medulloblastoma growth, could be the subject of future studies.

Discussion

Group 3 medulloblastoma has frequent c-*MYC* amplification and overexpression, is most likely to present with metastasis, and ultimately half of the patients die from recurrent disease.[22] In contrast, the rare Wnt subgroup presents a 5-year survival rate of 95%, while the SHH group and group 4 have 5-year survival rates of about 75%.[22] MBZ is a drug with a safe record in the pediatric population. We previously demonstrated the efficacy of MBZ in glioblastoma models, and this study indicates that MBZ is effective in models of 2 different molecular subtypes, including group 3, which is responsible for most patient deaths, and a vismodegib-resistant model. This is in line with the notion that the generally proposed cytotoxicity and anti-angiogenesis effect of MBZ is not restricted to a specific molecular group.

One proposed mechanism of MBZ-mediated cytotoxicity in parasites and tumor cells is the binding to tubulin and prevention of the formation of microtubule.[7,31] This has been the focus of our

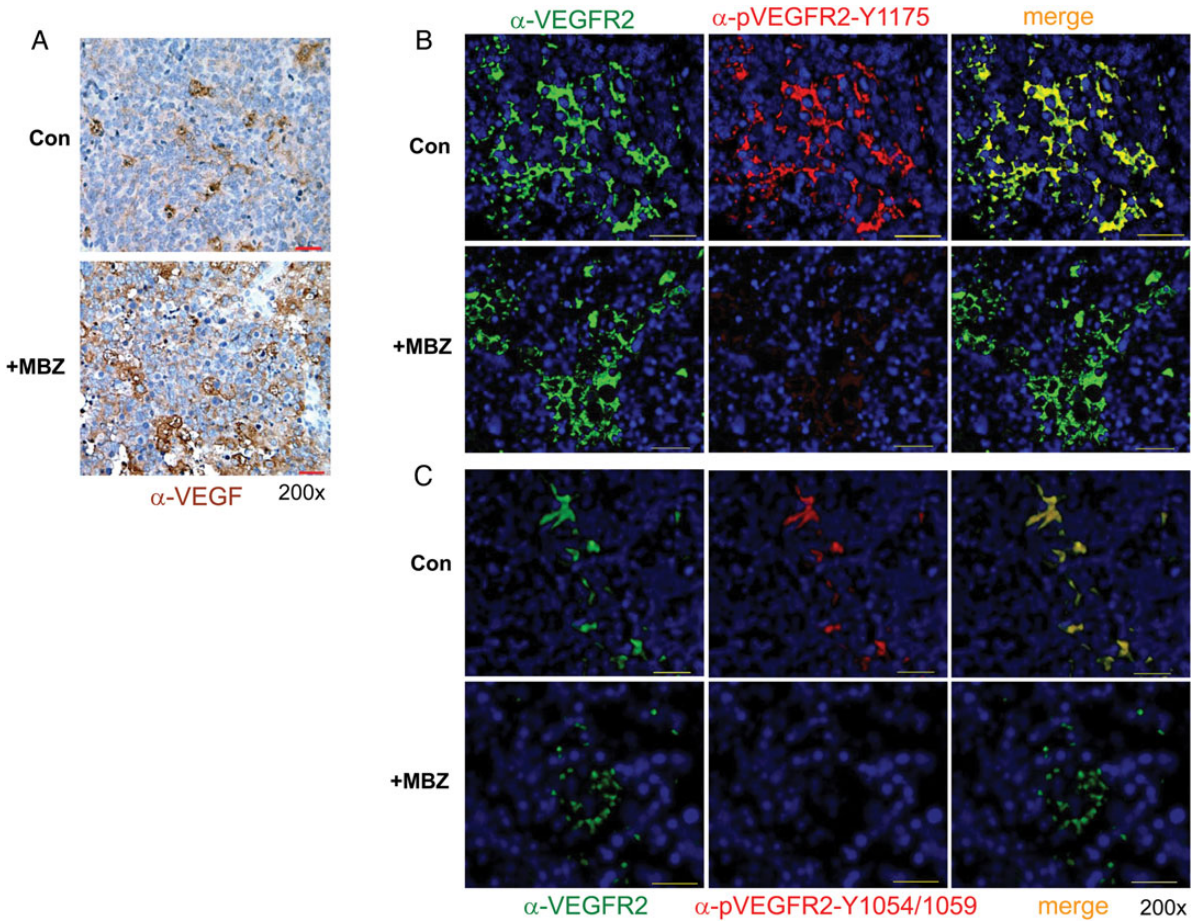

Fig. 6. MBZ inhibits VEGFR2 kinase activity in vivo. (A) Anti-VEGF immunohistochemistry staining of PTCH+/−, p53−/− medulloblastoma allografts treated or untreated with MBZ. VEGF was visualized by diaminobenzidine (brown), and the tissues were counterstained by hematoxylin (blue). All scale bars are 30 μm. (B, C) Anti-VEGFR2 (left panels, green) and anti-pVEGFR2-Y1175 (B) or anti-pVEGFR2-Y1054/1059 (C) (middle panels, red) staining of PTCH+/−, p53−/− medulloblastoma allografts untreated or treated with MBZ. The nuclei were visualized by DAPI staining (blue). MBZ treatment markedly reduced the autophosphorylation of VEGFR2-Y1175 and -Y1054/1059. The yellow color in the merged picture indicates the strong costaining of both antibodies in the control allografts. All pictures were taken with the setting of 800 msec exposure to green fluorescence, 1500 msec to Texas Red, and 200 msec to DAPI channel. All scale bars are 30 μm.

previous work, in which we primarily investigated the cytotoxic effect of MBZ in glioblastoma cells.[7] In this study, tubulin targeting of MBZ was evident in some of the medulloblastoma cells. In addition, a number of other mechanisms have been suggested for MBZ's antitumor activity. Recently, MBZ was investigated for its inhibition in a panel of tyrosine kinases relevant for tumorigenesis.[30] One group identified that MBZ was capable of inhibiting VEGFR2 in vitro.[11] This provided the hypothesis that VEGFR2 inhibition was perhaps contributing to the apparent lack of intratumoral bleeding and vasculature in MBZ-treated medulloblastoma allograft tumor, as we observed in Supplementary Fig. S2.

In this study, MBZ inhibited VEGFR2 autophosphorylation in medulloblastoma xenografts, in cultured HUVECs, and in a cell-free kinase assay with purified protein by competing with ATP binding. Consistent with VEGF-mediated angiogenesis, VEGF was expressed in the tumor tissue of the medulloblastoma model. The MBZ-treated medulloblastoma allografts and xenografts demonstrated significant reduction of tumor angiogenesis, while the microvessel density in the normal brain parenchyma was not noticeably affected. This is in line with the notion that VEGF is essential for tumor angiogenesis but less critical in maintenance of established normal blood vessels.[18,32,33] Bevacizumab, a monoclonal anti-VEGF antibody, has been widely used in glioblastoma and other cancers. Bevacizumab is able to reduce tumor vessel formation and brain edema, with relatively limited side effects and survival benefit as a single drug.[34,35] Therefore, clinical trials have been initiated in medulloblastoma patients with combined drug regimens, such as with bevacizumab and temsirolimus.[36] As such, one would suggest that drugs specifically targeting angiogenesis will have a better chance of success in combination with other therapeutics that are deliverable to the brain tumor.

In this context, MBZ holds the promise of attacking the brain tumor by multiple mechanisms as a single agent. Besides disrupting cellular structure by binding to tubulin,[7,37] MBZ also blocks VEGFR2 autophosphorylation and apparently inhibits tumor angiogenesis, and could also be inhibitory against other receptor or nonreceptor tyrosine kinases, which could significantly impair tumorigenic pathways.[30] In addition, it is likely that MBZ has multiple and complex antitumor effects. MBZ's medicinal benefits were first appreciated as a tubulin-binding agent, which affects directly cell proliferation and indirectly cellular signaling and could also further enhance the destruction of the proliferating endothelial cells in the neovasculatures. With several clinical trials of MBZ in adult high-grade glioma already establishing safe adult human dosing, MBZ is a promising candidate for a clinical trial in medulloblastoma patients. Given the high recurrence rate of medulloblastomas, MBZ's apparent ability to reach effective concentration in brain tumors, and its established safety in children, a reasonable starting point for clinical investigation would be patients with recurrent and treatment-refractory medulloblastoma.

Funding

This study was supported by the Accelerate Brain Cancer Cure Foundation; the Virginia and DK Ludwig Fund for Cancer Research; Generous support of Suzanne F. Cohen; the Irving J. Sherman Research Professorship in Neurosurgery to GJR; and the National Institute of Neurological Disorders and Stroke (R25NS065729) to V.S.

Supplementary material

Supplementary material is available at *Neuro-Oncology Journal* online (http://neuro-oncology.oxfordjournals.org/).

Conflict of interest statement. None declared.

References

1. Klesse LJ, Bowers DC. Childhood medulloblastoma: current status of biology and treatment. *CNS Drugs*. 2010;24(4):285–301.
2. Northcott PA, Jones DT, Kool M, et al. Medulloblastomics: the end of the beginning. *Nat Rev Cancer*. 2012;12(12):818–834.
3. Taylor MD, Northcott PA, Korshunov A, et al. Molecular subgroups of medulloblastoma: the current consensus. *Acta Neuropathol*. 2012; 123(4):465–472.
4. Rudin CM, Hann CL, Laterra J, et al. Treatment of medulloblastoma with hedgehog pathway inhibitor GDC-0449. *N Engl J Med*. 2009; 361(12):1173–1178.
5. Yauch RL, Dijkgraaf GJ, Alicke B, et al. Smoothened mutation confers resistance to a Hedgehog pathway inhibitor in medulloblastoma. *Science*. 2009;326(5952):572–574.
6. Bai RY, Staedtke V, Riggins GJ. Molecular targeting of glioblastoma: drug discovery and therapies. *Trends Mol Med*. 2011;17(6):301–312.
7. Bai RY, Staedtke V, Aprhys CM, et al. Antiparasitic mebendazole shows survival benefit in 2 preclinical models of glioblastoma multiforme. *Neuro Oncol*. 2011;13(9):974–982.
8. Chico LK, Van Eldik LJ, Watterson DM. Targeting protein kinases in central nervous system disorders. *Nat Rev Drug Discov*. 2009;8(11): 892–909.
9. Doudican NA, Byron SA, Pollock PM, et al. XIAP downregulation accompanies mebendazole growth inhibition in melanoma xenografts. *Anticancer Drugs*. 2013;24(2):181–188.
10. Doudican N, Rodriguez A, Osman I, et al. Mebendazole induces apoptosis via Bcl-2 inactivation in chemoresistant melanoma cells. *Mol Cancer Res*. 2008;6(8):1308–1315.
11. Dakshanamurthy S, Issa NT, Assefnia S, et al. Predicting new indications for approved drugs using a proteochemometric method. *J Med Chem*. 2012;55(15):6832–6848.
12. Keles GE, Berger MS, Srinivasan J, et al. Establishment and characterization of four human medulloblastoma-derived cell lines. *Oncol Res*. 1995;7(10–11):493–503.
13. Kim J, Aftab BT, Tang JY, et al. Itraconazole and arsenic trioxide inhibit Hedgehog pathway activation and tumor growth associated with acquired resistance to smoothened antagonists. *Cancer Cell*. 2012;23(1):23–34.
14. Munst GJ, Karlaganis G, Bircher J. Plasma concentrations of mebendazole during treatment of echinococcosis: preliminary results. *Eur J Clin Pharmacol*. 1980;17(5):375–378.
15. Bai RY, Koester C, Ouyang T, et al. SMIF, a Smad4-interacting protein that functions as a co-activator in TGFbeta signalling. *Nat Cell Biol*. 2002;4(3):181–190.
16. Bai RY, Staedtke V, Lidov HG, et al. OTX2 represses myogenic and neuronal differentiation in medulloblastoma cells. *Cancer Res*. 2012;72(22):5988–6001.
17. Weidner N. Current pathologic methods for measuring intratumoral microvessel density within breast carcinoma and other solid tumors. *Breast Cancer Res Treat*. 1995;36(2):169–180.

18. Goel HL, Mercurio AM. VEGF targets the tumour cell. *Nat Rev Cancer*. 2013;13(12):871–882.
19. Takahashi T, Yamaguchi S, Chida K, et al. A single autophosphorylation site on KDR/Flk-1 is essential for VEGF-A-dependent activation of PLC-gamma and DNA synthesis in vascular endothelial cells. *Embo J*. 2001;20(11):2768–2778.
20. Holmqvist K, Cross MJ, Rolny C, et al. The adaptor protein shb binds to tyrosine 1175 in vascular endothelial growth factor (VEGF) receptor-2 and regulates VEGF-dependent cellular migration. *J Biol Chem*. 2004;279(21):22267–22275.
21. Romer JT, Kimura H, Magdaleno S, et al. Suppression of the Shh pathway using a small molecule inhibitor eliminates medulloblastoma in Ptc1(+/−)p53(−/−) mice. *Cancer Cell*. 2004; 6(3):229–240.
22. Northcott PA, Korshunov A, Pfister SM, et al. The clinical implications of medulloblastoma subgroups. *Nat Rev Neurol*. 2012;8(6):340–351.
23. Adamson DC, Shi Q, Wortham M, et al. OTX2 is critical for the maintenance and progression of Shh-independent medulloblastomas. *Cancer Res*. 2010;70(1):181–191.
24. Bai R, Siu IM, Tyler BM, et al. Evaluation of retinoic acid therapy for OTX2-positive medulloblastomas. *Neuro Oncol*. 2010;12(7): 655–663.
25. Cheng SY, Nagane M, Huang HS, et al. Intracerebral tumor-associated hemorrhage caused by overexpression of the vascular endothelial growth factor isoforms VEGF121 and VEGF165 but not VEGF189. *Proc Natl Acad Sci U S A*. 1997;94(22):12081–12087.
26. Jung S, Moon KS, Jung TY, et al. Possible pathophysiological role of vascular endothelial growth factor (VEGF) and matrix metalloproteinases (MMPs) in metastatic brain tumor-associated intracerebral hemorrhage. *J Neurooncol*. 2006;76(3):257–263.
27. Chung AS, Lee J, Ferrara N. Targeting the tumour vasculature: insights from physiological angiogenesis. *Nat Rev Cancer*. 2010; 10(7):505–514.
28. Jin Kim Y, Hyun Kim C, Hwan Cheong J, et al. Relationship between expression of vascular endothelial growth factor and intratumoral hemorrhage in human pituitary adenomas. *Tumori*. 2011;97(5): 639–646.
29. Baluk P, McDonald DM. Markers for microscopic imaging of lymphangiogenesis and angiogenesis. *Ann N Y Acad Sci*. 2008; 1131:1–12.
30. Nygren P, Fryknas M, Agerup B, et al. Repositioning of the anthelmintic drug mebendazole for the treatment for colon cancer. *J Cancer Res Clin Oncol*. 2013;139(12):2133–2140.
31. Kohler P. The biochemical basis of anthelmintic action and resistance. *Int J Parasitol*. 2001;31(4):336–345.
32. Argraves WS, Larue AC, Fleming PA, et al. VEGF signaling is required for the assembly but not the maintenance of embryonic blood vessels. *Dev Dyn*. 2002;225(3):298–304.
33. Lijnen HR, Scroyen I. Effect of vascular endothelial growth factor receptor 2 antagonism on adiposity in obese mice. *J Mol Endocrinol*. 2013;50(3):319–324.
34. von Baumgarten L, Brucker D, Tirniceru A, et al. Bevacizumab has differential and dose-dependent effects on glioma blood vessels and tumor cells. *Clin Cancer Res*. 2011;17(19):6192–6205.
35. Narita Y. Drug review: Safety and efficacy of bevacizumab for glioblastoma and other brain tumors. *Jpn J Clin Oncol*. 2013;43(6): 587–595.
36. Piha-Paul SA, Shin SJ, Vats T, et al. Pediatric patients with refractory central nervous system tumors: experiences of a clinical trial combining bevacizumab and temsirolimus. *Anticancer Res*. 2014; 34(4):1939–1945.
37. Sasaki J, Ramesh R, Chada S, et al. The anthelmintic drug mebendazole induces mitotic arrest and apoptosis by depolymerizing tubulin in non-small cell lung cancer cells. *Mol Cancer Ther*. 2002;1(13):1201–1209.